

# Endometrial Epithelial Cell Apoptosis Is Inhibited by a ciR8073-miR181a-Neurotensin Pathway during Embryo Implantation

Lei Zhang,<sup>1,2</sup> Xiaorui Liu,<sup>1,2</sup> Sicheng Che,<sup>1,2</sup> Jiuzeng Cui,<sup>1</sup> Xingna Ma,<sup>1</sup> Xiaopeng An,<sup>1</sup> Binyun Cao,<sup>1</sup> and Yuxuan Song<sup>1</sup>

<sup>1</sup>College of Animal Science and Technology, Northwest A&F University, Yangling, Shaanxi 712100, P.R. China

**Development of the receptive endometrium (RE) from the pre-receptive endometrium (PE) is essential for embryo implantation, but its molecular mechanisms have not been fully understood. In this study, lncRNA-miRNA-mRNA and circRNA-miRNA-mRNA networks were constructed to explore the functions of potential competing endogenous RNAs (ceRNA) during the development of RE in dairy goats. We observed that circRNA8073 (ciR8073) decreased the levels of miR-181a by acting as a miRNA sponge. This effect indirectly increased the expression of neurotensin in endometrial epithelial cells (EECs). Neurotensin then inhibited EEC apoptosis by increasing the expression of BCL-2/BAX in favor of BCL-2 via the MAPK pathway and also induced increased expression of leukemia-inhibitory factor, cyclo-oxygenase 2, vascular endothelial growth factor A, and homeobox A10. We have thus identified a ciR8073-miR181a-neurotensin pathway in the endometrium of dairy goats. Through this pathway, ciR8073 functions as a ceRNA that sequesters miR-181a, thereby protecting neurotensin transcripts from miR-181a-mediated suppression in EECs.**

## INTRODUCTION

The establishment of endometrial receptivity is known as the “window of implantation” (WOI), which is a spatially and temporally restricted stage.<sup>1</sup> During this period, the endometrium undergoes pronounced structural and functional changes that prepare it to be receptive to adhesion by the qualified embryo.<sup>2</sup> An abnormal receptive endometrium (RE) is one of the major reasons for the failure of embryo transplantation during assisted reproduction with good-quality embryos.<sup>3</sup> Notably, many studies have reported that attaining endometrial receptivity is a complex process involving numerous molecular mediators.<sup>1</sup>

It has been speculated that non-coding RNAs (ncRNAs) serve as key regulators of gene expression under physiological and pathological conditions.<sup>4</sup> These include miRNAs, long non-coding RNAs (lncRNAs), and circular RNAs (circRNAs; a class of RNAs derived mostly from non-canonical splicing in which the exon ends are joined to form a loop).<sup>5,6</sup> ncRNAs are reportedly crucial for a variety of physiological processes, including the establishment of endometrial receptivity.<sup>7-9</sup>

lncRNAs and circRNAs contain miRNA response elements (MREs) and compete with mRNAs for MREs. This enables them to act as molecular sponges for miRNAs and ultimately de-repress miRNA target genes<sup>10</sup> to influence the post-transcriptional regulation. The competing endogenous RNA (ceRNA) hypothesis suggests that a non-coding function of any uncharacterized RNA transcript can be predicted by the identification of putative miRNA binding sites. This hypothesis is now supported by experimental evidence for an accumulating number of lncRNAs<sup>11-13</sup> and circRNAs.<sup>14,15</sup> For example, lncRNA-MIAT effectively decreases the expression of miR-150-5p and the target gene *VEGF*,<sup>11</sup> lncRNA-CCAT1 increases *Bmi1* expression by competitively sponging miRNA-218-5p,<sup>12</sup> and lncRNA-MD1 acts as a miR-133 and miR-135 sponge.<sup>13</sup> Although the function of most circRNAs remains elusive, at least three circRNAs have been experimentally shown to act as ceRNAs: ciRS-7 inhibits miR-7 activity in the CNS,<sup>15</sup> a Sry-derived circRNA acts as a sponge for miR-138,<sup>14</sup> and ciR-ITCH controls the level of itchy E3 ubiquitin protein ligase by sponging miR-7, miR-17, and miR-214 in esophageal squamous cell carcinoma.<sup>16</sup>

The reported results outlined above suggest that a better understanding of ceRNAs could provide new insight into the mechanisms of RE. Our findings here contribute to a better understanding of the molecular regulation of RE and may provide essential information in support of further research on the development of endometrial receptivity.

## RESULTS

### Differentially Expressed miRNA, mRNA, lncRNA, and circRNA between the RE and PE in Dairy Goat

In our previous study, a total of 145 differentially expressed miRNAs (DEmiRs) with *p* values < 0.05 and fold changes > 2

Received 22 June 2018; accepted 6 December 2018;

<https://doi.org/10.1016/j.omtn.2018.12.005>.

<sup>2</sup>These authors contributed equally to this work.

**Correspondence:** Yuxuan Song, College of Animal Science and Technology, Northwest A&F University, No. 22 Xinong Road, Yangling, Shaanxi 712100, P.R. China.

**E-mail:** [yuxuan\\_song2016@163.com](mailto:yuxuan_song2016@163.com)

**Correspondence:** Binyun Cao, College of Animal Science and Technology, Northwest A&F University, No. 22 Xinong Road, Yangling, Shaanxi 712100, P.R. China.

**E-mail:** [binyun\\_cao@163.com](mailto:binyun_cao@163.com)



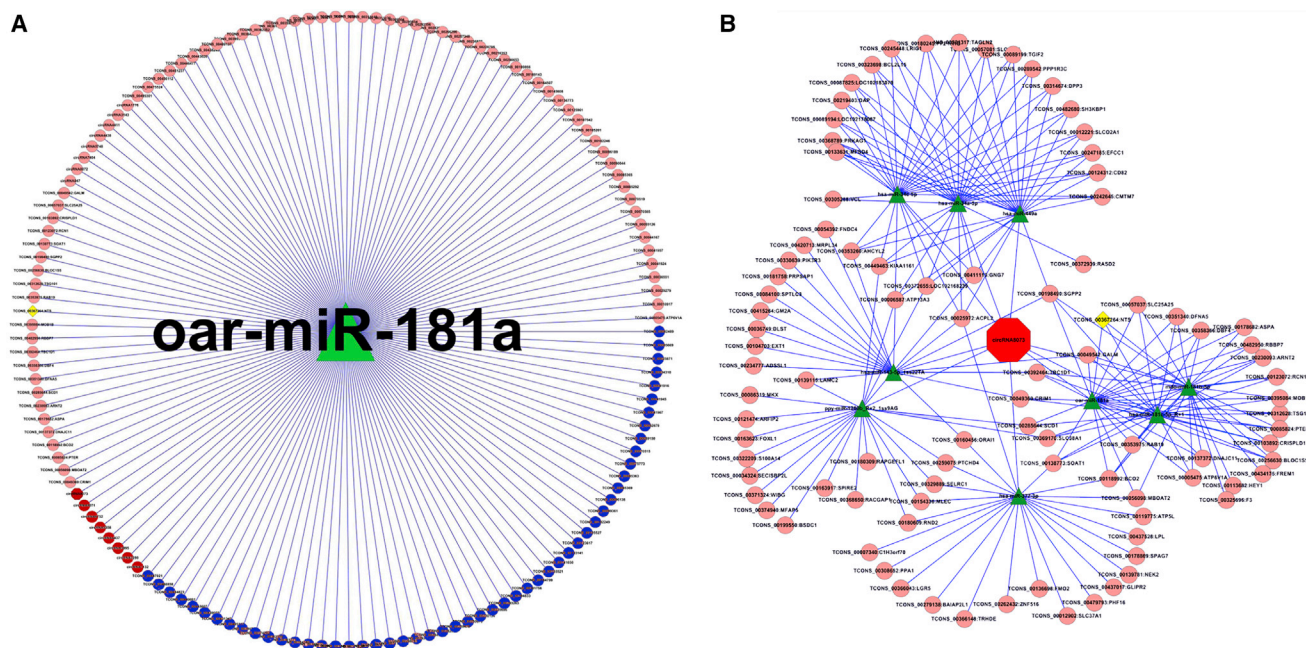


**Figure 1. The ceRNA Network Centered on miR-181a and ciR8073 in Endometrium of Dairy Goats**

(A) The differentially expressed targets of miR-181a; (B) the ceRNA network centered on ciR8073. Red hexagon, ciR8073; yellow diamond, NTS; green triangle, miRNAs; red circle, circRNAs; blue circle, lncRNAs; pink circle, mRNAs.

(Data S1), including 111 upregulated and 34 downregulated DEmiRs, were identified in the RE compared with the pre-receptive endometrium (PE).<sup>8</sup> Moreover, miR-181a had a high expression level, which decreased 0.38-fold in the RE compared with the PE.

Additionally, 810 mRNAs were found to differ significantly between the PE and RE, and the full list of differentially expressed mRNA (DEmR) with  $p$  values  $< 0.05$  and fold changes  $> 2$  is provided in Data S2. *NTS* mRNA levels decreased 6.08-fold in the RE compared with the PE in dairy goats, but this result was inconsistent with previous results, where *NTS* was remarkably increased in the RE.<sup>17</sup> Furthermore, a total of 668 differentially expressed lncRNAs (DElncRs) were found (Data S3), and TCONS\_00376915 (lncR915) was significantly higher in the RE compared with the PE. There were 334 differentially expressed circRNAs (DEciRs) (Data S4), of which 77 were upregulated and 257 were downregulated in the RE compared with the PE. Notably, ciR8073 was highly and specifically expressed in the RE.

#### Prediction of miRNA Binding Sites and Construction of ceRNA Network

To examine the molecular mechanism of ncRNAs involved in the development of the RE, all possible interactions of each DEmiR with all DEmRs (Data S5), DElncRs (Data S6), and DEciRs (Data S7) were analyzed using Targetscan and miRanda. As a result, *NTS*, lncRNA915 (lncR915), and ciR8073 were predicted as a target of miR-181a.

Based on the theory of ceRNA, the DEmiR-DEmR, DEmiR-DEciR, and DEmiR-DElncR pairs were used to construct the ceRNA networks. As shown in Data S8, 144 DEmiRs shared 239,385 MREs with 305 DEmRs, 105 DEciRs, and 887 DElncRs in the ceRNA network. The ceRNA networks were visualized by importing the above interactions into the Cytoscape software to assemble the regulation network. For example, miR-181a shared MREs with 24 DEmRs, 105 DEciRs, and 16 DElncRs in the ceRNA network (Figure 1A; Data S9). Notably, ciR8073 shared MREs with nine DEmiRs, including miR-181a (Figure 1B; Data S10). As described above, the regulatory role of ncRNAs in the RE was very complicated and warrants an in-depth study in the future.

To explore the function of the ceRNA network, the interrelated genes within the network were imported with the Gene Ontology (GO) terms and Kyoto Encyclopedia of Genes and Genomes (KEGG) pathways. Based on the GO enrichment analysis, 755 GO functions were found to be the significant components relating the genes in the network, involved in processes such as regulation of cell growth (GO: 0001558), cell differentiation (GO: 0030154), multicellular organismal development (GO: 0007275), cell-cell signaling (GO: 0007267), apoptosis (GO: 0006915), focal adhesion (GO: 0005925), and metalloproteinase activity (GO: 0008237) (Data S11; Figure S1A). Analysis of the functional pathways demonstrated that the ceRNA network potentially modulated multiple signaling pathways, such as focal adhesion (ko04510), the mammalian target of rapamycin (mTOR) signaling pathway (ko04150), the insulin signaling pathway (ko04910), the neurotrophin signaling pathway (ko04722), and apoptosis (ko04210) (Data S12; Figure S1B).

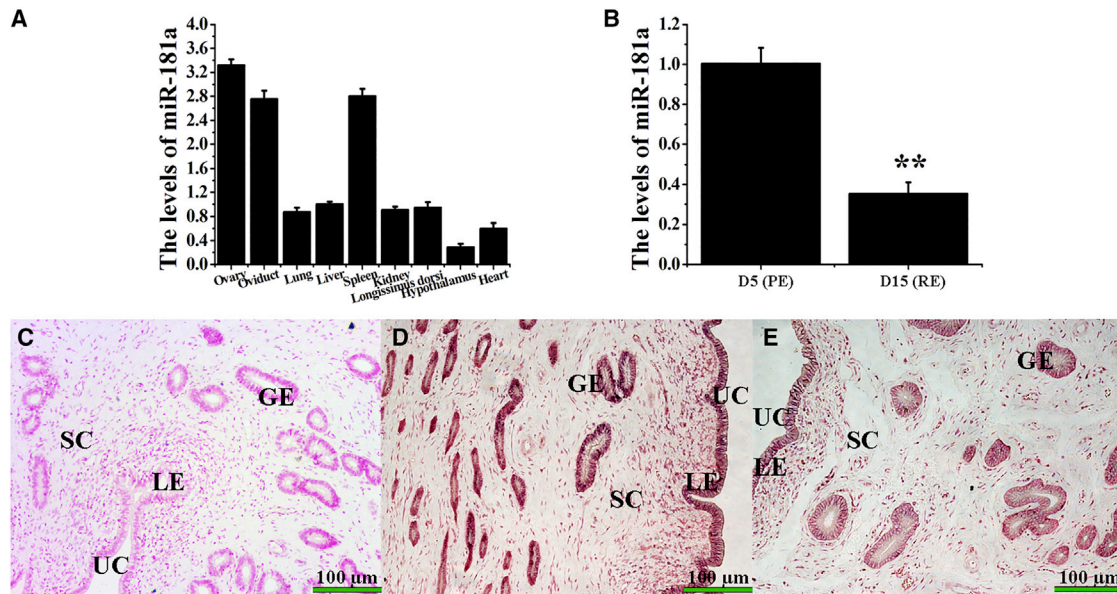


**Figure 2. miR-181a Was Significantly Decreased in RE Compared with PE**

(A) The miR-181a was expressed in various tissues of dairy goats; (B) the miR-181a levels in endometrium in PE and RE. The miR-181a levels were measured by stem-loop qRT-PCR and normalized to U6; the values are shown as means  $\pm$  SD ( $n = 3$ ); \*\* $p < 0.01$ , \* $p < 0.05$ . (C) The NC for *in situ* hybridization; the miR-181a in the endometrium in PE (D) and RE (E) were detected by *in situ* hybridization. UC, uterine cavity; LE, luminal epithelium; GE, glandular epithelium; SC, stroma cell. Original magnification  $\times 200$ ; scale bars, 100  $\mu\text{m}$ .

#### miR-181a and NTS Were Differentially Expressed in the PE and RE

Stem-loop qRT-PCR was used to validate the expression levels of miR-181a in various tissues of dairy goats, and the results showed that it was expressed ubiquitously (Figure 2A). The highest expression level was observed in the ovary, followed (in order) by the spleen, oviduct, liver, longissimus dorsi, kidney, lungs, heart, and hypothalamus. In the endometrium of dairy goats, the expression level of miR-181a in the RE was lower than that in the PE (Figure 2B). The miRNA *in situ* hybridization (MISH) assay further revealed that miR-181a was significantly decreased in the RE compared with the PE (Table 1), especially in the endometrial epithelial cells (Figures 2C–2E).

NTS was widely expressed in a series of tissues, and the lowest expression levels were observed in the ovary, and increased expression was observed (in order) in the oviduct, lung, liver, spleen, kidney, longissimus dorsi, hypothalamus, and heart (Figure 3A). Furthermore, the expression level of NTS increased 195-fold in the endometrium in the RE compared to the PE (Figure 3B), which was consistent with previously reported sequencing data.<sup>17</sup> Immunohistochemistry (IHC) results further showed that the NTS protein was upregulated in the RE (Table 2), especially in the EECs (Figures 3C–3F).

#### The Levels of miR-181a and NTS mRNA Were Affected by E2 and P4 in EECs *In Vitro*

To investigate the response of miR-181a and NTS levels to sex hormones in EECs *in vitro*, estrogen (E2) and progesterone (P4) were diluted in cell medium to different concentrations. The results

showed that miR-181a levels were significantly decreased in a concentration-dependent manner in the presence of E2 alone and enhanced in the presence of P4 alone in EECs (Figure 4A). Furthermore, the highest levels were observed with 20 ng/mL P4 alone, and the lowest levels were observed with 100 pg/mL E2 alone, suggesting that E2 decreased but P4 increased the miR-181a levels in EECs *in vitro*. Furthermore, E2 and P4 also regulated the NTS mRNA levels but without obvious regularity in EECs *in vitro*, and the highest levels appeared when a combination of 100 pg/mL E2 and 20 ng/mL P4 were used (Figure 4B).

#### NTS Expression Was Downregulated by miR-181a in EECs *In Vitro*

Transfection of miR-181a mimics successfully led to a greater than 168-fold increase, whereas miR-181a inhibitors led to a 0.39-fold decrease in EECs (Figure S2A). To determine whether miR-181a directly targeted goat NTS through the predicted binding sites in the NTS 3' UTR, the psiCHECK-2 reporter and mutated plasmids were constructed (Figure 5A). The luciferase activity of the miR-181a group was significantly lower than that of the negative control (NC) group ( $p < 0.01$ ), but these reductions were not observed with the mutated plasmid (Figure 5B).

The NTS mRNA levels decreased in EECs after transfection with miR-181a mimics ( $p < 0.05$ ), whereas, miR-181a inhibitors increased the NTS mRNA levels ( $p < 0.01$ ; Figure 5C) in EECs *in vitro*. NTS protein levels were evaluated by western blot (WB) analysis, and the quantification of protein expression is shown in Figure 5D, demonstrating

**Table 1. MISH Staining Results of miR-181a in the Uterus of Dairy Goats**

Index	Area		Density		IOD	
	Mean	Sum	Mean	Sum	Mean	Sum
PE (D5)	758.416	1,623,011	0.156	333.794	210.80	451,112.63
RE (D15)	160.026*	189,631**	0.204	242.259	33.922**	40,197.79*

MISH, miRNA *in situ* hybridization; IOD, integrated optical density. \* $p < 0.05$ , \*\* $p < 0.01$ .

that the NTS protein was significantly decreased in miR-181a-transfected cells compared with the NC ( $p < 0.05$ ; Figure 5D). Additionally, miR-181a inhibitors significantly increased the NTS protein in EECs ( $p < 0.05$ ; Figure 5D). Thus, these results suggested that goat NTS was a target of miR-181a in EECs.

#### miR-181a Did Not Regulate lncR915 in EECs *In Vitro*

Transfection with pcDNA3.1(+)-lncR915 successfully led to an 89-fold increase of lncR915 in EECs *in vitro* ( $p < 0.01$ ; Figure S2B). The psiCHECK-2 reporter and mutated plasmids were constructed (Figure 6A), and the luciferase activity of the miR-181a mimics and inhibitor groups did not significantly change compared to the NC group ( $p > 0.05$ ; Figure 6B). Furthermore, there was no significant change in the expression levels of lncR915 (Figure 6C) in EECs that were treated with miR-181a mimics and inhibitors. In addition, lncR915 did not change the miR-181a (Figure 6D) and NTS mRNA levels (Figure 6E) in EECs. Thus, these results suggested that miR-181a did not regulate lncR915 in the EECs of dairy goats.

#### ciR8073 Served as a miR-181a Sponge in EECs *In Vitro*

Transfection with pcDNA3.1(+)-ciR8073 resulted in a 27.57-fold increase of ciR8073 compared with NC in EECs *in vitro* ( $p < 0.01$ ; Figure S2C). To determine whether miR-181a directly targeted ciR8073 through the predicted binding sites, the psiCHECK-2 reporter and mutated plasmids were constructed (Figure 7A), and the luciferase activity of the miR-181a mimics group was significantly lower than that of the NC group ( $p < 0.01$ ), whereas these reductions were not observed with the mutated plasmids ( $p > 0.05$ ; Figure 7B).

Furthermore, the level of ciR8073 decreased significantly when the cells were treated with miR-181a mimics (Figure 7C), and the miR-181a level was also decreased by ciR8073 in EECs (Figure 7D). On the contrary, the level of NTS mRNA was significantly increased when ciR8073 was overexpressed and decreased when ciR8073 was mutated in EECs *in vitro* (Figure 7E). Furthermore, the expression levels of NTS were increased by ciR8073, and this increase was counteracted by miR-181a at both the mRNA and protein levels (Figures 7E–7G). Thus, these results suggested that miR-181a targeted ciR8073, thereby demonstrating the accuracy of the ciR8073-miR-181a-NTS network interaction.

#### miR-181a Promoted Cell Apoptosis of EECs *In Vitro*

Methyl thiazolyl tetrazolium (MTT) assays were used to demonstrate that miR-181a mimics inhibited the proliferation of EECs (Figure 8A;  $p < 0.05$ ), whereas the miR-181a inhibitor promoted the proliferation

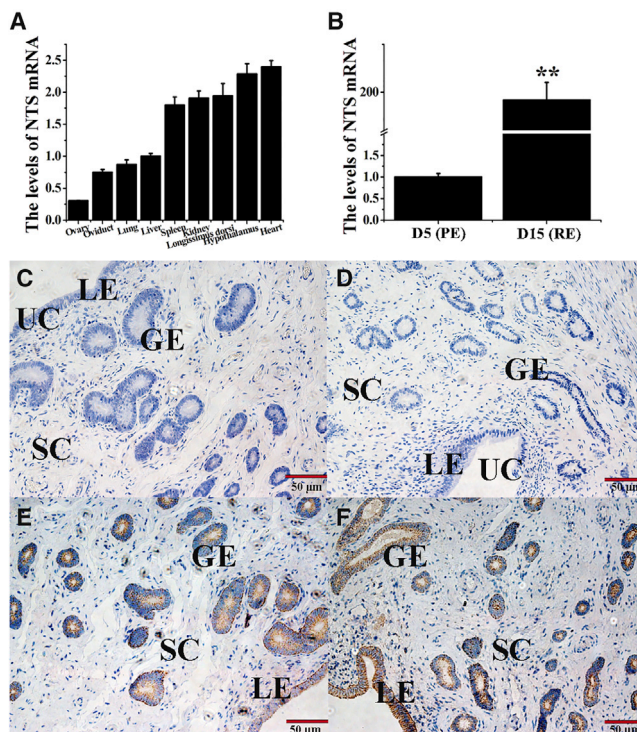


**Figure 3. NTS Was Significantly Increased in RE Compared with PE**

(A) The NTS was expressed in various tissues of dairy goats; (B) the NTS levels in endometrium in PE and RE. The NTS levels were measured by qRT-PCR and normalized to GAPDH; the values are shown as means  $\pm$  SD ( $n = 3$ ). \*\* $p < 0.01$ , \* $p < 0.05$ . (C and D) The NC for immunohistochemical staining in PE (C) and RE (D); NTS levels were detected by immunohistochemical staining in the endometrium in PE (E) and RE (F). LE, luminal epithelium; GE, glandular epithelium; SC, stroma cell. Original magnification  $\times 100$ ; scale bars, 50  $\mu$ m.

of EECs ( $p < 0.05$ ). Flow cytometry (FCM) was used to analyze the changes in the cell cycle, demonstrating that the numbers of cells in S phase was higher in EECs treated with the miR-181a mimics compared to the NC (Figures 8B and S3). Furthermore, an Annexin-V-fluorescein isothiocyanate (FITC)/PI assay combined with FCM was used to detect the effects of miR-181a on cell apoptosis, demonstrating that miR-181a induced the apoptosis of EECs ( $p < 0.01$ ; Figure 8C), whereas the miR-181a inhibitor inhibited apoptosis ( $p < 0.05$ ; Figure S4).

The BCL-2 expression levels were decreased significantly by miR-181a mimics and increased significantly by inhibitors ( $p < 0.05$ ; Figure 8D). On the contrary, the BAX protein levels were increased and decreased by miR-181a mimics and inhibitors, respectively ( $p < 0.05$ ; Figure 8D). Furthermore, miR-181a mimics facilitated the phosphorylation of JNK (p-JNK) and increased the levels of P27, whereas miR-181a inhibitors decreased the levels of P27 and phosphatidylinositol 3-kinase (PI3K) ( $p < 0.05$ ; Figure 8D).

In addition, the changes in LIF, COX2, VEGFA, HOXA10, and osteopontin (OPN) protein levels were investigated in endometrial cells

**Table 2. ISH Staining Results of NTS in the Uterus of Dairy Goats**

Index	Area		Density		IOD	
	Mean	Sum	Mean	Sum	Mean	Sum
PE (D5)	76.71	181,276	0.296	699.196	21.410	50,592.813
RE (D15)	72.699	151,650	0.432*	900.430	32.879*	68,585.008*

ISH, *in situ* hybridization; IOD, integrated optical density. \* $p < 0.05$ .

after the cells were treated with miR-181a mimics or inhibitors. The LIF and COX2 protein levels were increased in EECs treated with miR-181a mimics ( $p < 0.05$ ) and decreased in the inhibitor group ( $p < 0.05$ ; Figure 8D). However, the opposite results were observed for the OPN protein levels, which suggested that miR-181a inhibited OPN in EECs *in vitro* ( $p < 0.05$ ; Figure 8D).

#### NTS-Inhibited Cell Apoptosis of EECs *In Vitro*

To further investigate the function of NTS in EECs, the overexpression vector pcDNA3.1(+)-NTS was constructed and small interfering RNA (siRNA)-NTS was synthesized, and NTS was overexpressed or inhibited successfully in EECs *in vitro* (Figure S5). In addition, the levels of miR-181a decreased and increased due to NTS and siRNA-NTS, respectively (Figure S6), suggesting a negative relationship between NTS and miR-181a in EECs.

The MTT assay showed that overexpression of NTS markedly promoted proliferation of EECs ( $p < 0.05$ ; Figure 9A), whereas siRNA-NTS significantly inhibited proliferation of EECs ( $p < 0.05$ ; Figure 9D). No notable change was observed in the analysis of cell cycle ( $p > 0.05$ ; Figures 9B and 9E), but overexpression of NTS inhibited EEC apoptosis ( $p < 0.05$ ; Figure 9C), whereas siRNA-NTS dramatically induced EEC apoptosis ( $p < 0.05$ ; Figures 9F, S6, and S7). Thus, some apoptosis-related genes were detected when NTS was overexpressed in EECs, and the results showed that NTS increased the protein levels of BCL-2, Caspase-8, FAS, and pleiotrophin (PTN), and decreased BAX and Sp1 transcription factor (SP1) ( $p < 0.05$ ; Figure 10). In addition, NTS also increased p-ERK1/2, JNK, p-JNK, and p-P38 but decreased the total level of JNK. At the same time, NTS decreased the protein levels of P27 and PI3K ( $p < 0.05$ ; Figure 10). Furthermore, the protein levels of BCL-2 and BAX were also detected in EECs when NTS was silenced by siRNA-NTS, and the results showed that BCL-2 and BAX were downregulated and upregulated, respectively (Figure S9). These results were in accordance with the function of miR-181a but contrary to what was observed when NTS was overexpressed in EECs *in vitro*. All these results suggested that miR-181a induced EECs apoptosis by targeted NTS.

Finally, we analyzed the expressions of biochemical endometrial receptivity biomarkers. WB analysis revealed that NTS induced an increase in LIF, COX2, VEGFA, and HOXA10 ( $p < 0.05$ ; Figure 10). In addition, the endometrial receptivity biomarkers were detected in EECs when NTS was knocked out by siRNA-NTS, and the results showed that siRNA-NTS resulted in an increase in the VEGFA levels in EECs *in vitro* (Figure S10).

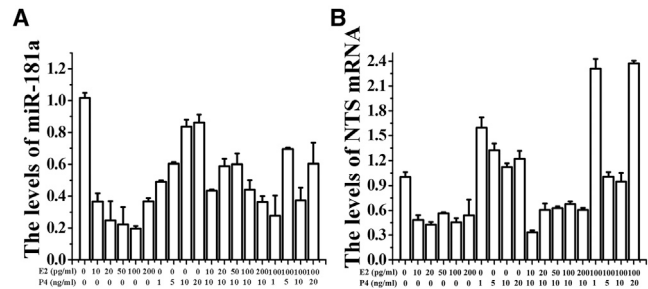


**Figure 4. E2 and P4 Regulated the Expression Levels of miR-181a and NTS in EECs**

(A) The levels of miR-181a; (B) the levels of NTS mRNA. The values are shown as means  $\pm$  SD ( $n = 3$ ).

#### DISCUSSION

Previous studies have revealed that ceRNAs could serve as post-transcriptional regulators of protein-coding gene expression by sequestering miRNAs from other target transcripts, such as lncRNAs, mRNAs, pseudogenes, and circRNAs.<sup>18,19</sup> In this study, based on the high-throughput RNA-sequencing data, we constructed putative ceRNA networks by integrating lncRNAs, circRNAs, mRNAs, and miRNAs in the endometrium of dairy goats. This is the first study to comprehensively identify ncRNAs in the development of the RE from the PE by regulatory network analysis. Notably, ciR8073 shared MREs with nine DE miRs, including miR-181a. Furthermore, miR-181a shared MREs with 24 mRNAs, 105 circRNAs, and 16 lncRNAs in the ceRNA networks, and NTS mRNA, ciR8073, and lncR915 shared the same MRE as miR-181a.

In pigs, miR-181a was found to be highly expressed on day 15 of gestation, followed by decreased expression on gestational days 26 and 50 in the endometrium during pregnancy.<sup>20</sup> Furthermore, miR-181a could promote human endometrial stromal cells (hESCs) decidualization-related gene expression and morphological transformation; conversely, inhibition of miR-181a expression compromised hESC decidualization *in vitro*.<sup>21</sup> In addition, the higher expression levels of NTS in the endometrial epithelial and glandular epithelial cells were detected in the bovine endometrium and were more abundant in the endometrium from summer than that from autumn.<sup>22</sup> In this study, miR-181a directly inhibited NTS expression levels at the mRNA and protein levels via its 3' UTR in EECs of dairy goats.

Hansen identified a highly expressed ciRS-7 that contained more than 70 selectively conserved miRNA target sites, markedly suppressed miR-7 activity, resulting in increased levels of miR-7 targets.<sup>14</sup> In EECs of dairy goats, ciR8073 displayed a sponging effect for miR-181a, and the NTS levels were significantly increased when ciR8073 was overexpressed and decreased when ciR8073 was mutated in EECs, suggesting a high degree of endogenous interaction. To our knowledge, this study served as the first functional analysis of a naturally expressed circRNA in dairy goats.

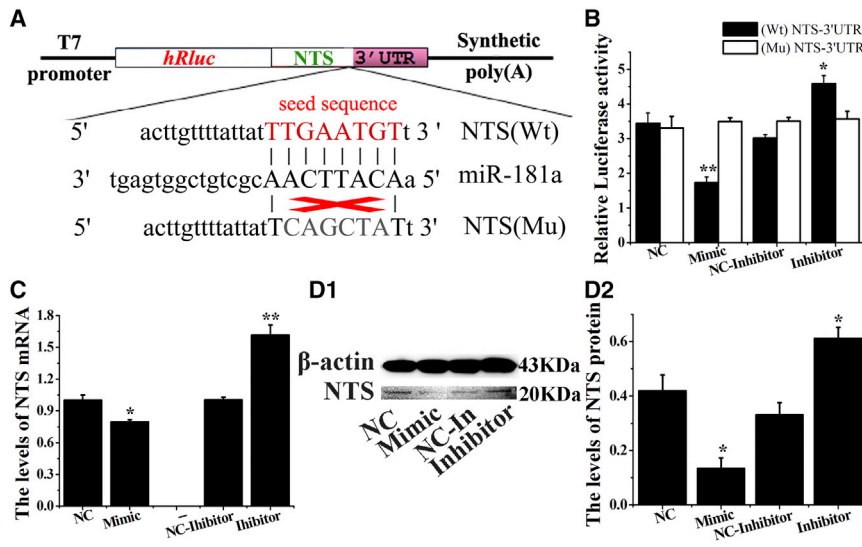


**Figure 5. miR-181a Downregulated the Expression Level of NTS via the 3' UTR**

(A) Schematic diagram illustrating the design of luciferase reporters with the WT-NTS 3' UTR (Wt-NTS) or the site-directed mutant NTS 3' UTR (Mu-NTS). The nucleotides in red represent the "seed sequence" of miR-181a; the mutation nucleotides are in gray. (B) The NTS-3' UTR luciferase reporter vectors were co-transfected with miR-181a mimic (or negative control) into 293T cells; luciferase assay was performed 24 h after transfection. (C) miR-181a downregulated the NTS mRNA levels in EEC; NTS mRNA levels were measured by qRT-PCR and normalized to GAPDH. (D) NTS protein levels in EECs were measured by WB, and the densitometry was normalized to the  $\beta$ -actin density from the same lane. Each experiment was repeated three times in triplicate; the results are represented as mean  $\pm$  SD ( $n = 3$ ). \* $p < 0.05$ , \*\* $p < 0.01$ .

In many mammals, endometrial cells were remodeled by apoptosis and proliferation throughout the estrous cycle,<sup>23</sup> and studies had been performed in humans,<sup>24</sup> mice,<sup>25</sup> and pigs.<sup>26</sup> Furthermore, a coordinated regulation of the embryonic induction of EEC apoptosis was crucial for the embryo to breach the epithelial barrier *in vitro*.<sup>27</sup>

In this study, miR-181a promoted EEC apoptosis, and a further study showed that miR-181a resulted in a decreased of BCL-2 and increased of BAX, consistent with a previous study that reported that miR-181a could directly target BCL-2 in endothelial cells.<sup>28</sup> Furthermore, miR-181a increased p-JNK and P27, and these results suggested that miR-181a may play an important role as an apoptosis-regulatory factor via the MAPK pathway in EECs of dairy goat.

Recently, several morphological and biochemical biomarkers of endometrial receptivity were proposed, including LIF, COX2, VEGFA, HOXA10, and OPN. LIF was observed in the cytoplasm of EECs<sup>29</sup> and has been widely acknowledged as biochemical markers of the RE.<sup>30</sup> COX2 was a rate-limiting enzyme for the synthesis of prostaglandin, which was a critical factor for maintaining the uterine environment during early pregnancy,<sup>31</sup> and we found that the COX2 protein levels were decreased by miR-181a in EECs. In addition, VEGFA was expressed in the mouse and rabbit endometrium and likely contributed to the increased angiogenesis and vascular permeability necessary for implantation.<sup>32,33</sup> Evidence suggests that the expression of VEGFA is highly regulated in a temporal and spatial manner at the early stage of implantation.<sup>34</sup> HOXA10, a homeobox-containing transcription factor, was expressed cyclically during the menstrual cycle in the endometrium under the influence of steroid hormone and had the highest expression level during the WOI.<sup>35,36</sup> OPN played an important role in endometrial receptivity due to its consistent upregulation during the WOI.<sup>37</sup> In this study, miR-181a significantly increased LIF and COX2 protein levels but decreased the levels of OPN in EECs *in vitro*. These results suggested that miR-181a might participate in the formation of endometrial receptivity.

NTS was detected in the bovine endometrium, and the expression levels showed differences between the breeding and non-breeding seasons.<sup>22</sup> However, there has been no relevant literature on the function of NTS in the formation of endometrial receptivity in dairy goats, and this study was the first to investigate the function of NTS in EECs of dairy goats. In the present study, we determined that NTS could promote the proliferation of EECs and inhibit cell apoptosis *in vitro*; however, NTS did not affect the protein level of Caspase-8 but did increase the protein level of Caspase-3 in EECs. In addition, NTS did not affect the protein levels of FAS, which is a critical factor for the progression of extrinsic apoptosis in the human endometrium.<sup>24,38</sup>

Iwahori et al.<sup>39</sup> reported that SP1 might play a role in DNA repair at damage sites and inhibit cell apoptosis, and NTS dramatically decreased the SP1 protein levels in EECs, which was consistent with the FCM results. PTN is a secreted cytokine that participates in diverse biology process, such as cell adhesion, migration, survival, growth, and differentiation.<sup>40</sup> In this study, the protein levels of PTN increased with the increase of NTS in EECs. Since PTN was mainly expressed in the caruncular areas of the bovine endometrium,<sup>41</sup> it might also participate in the proliferation of endometrial cells in dairy goats. Further investigation revealed that NTS decreased the total levels of MAPK and JNK but increased the phosphorylation levels of MAPK, JNK, and P38. Meanwhile, NTS decreased the protein levels of P27 and PI3K in EECs *in vitro*. Additionally, NTS could inhibit apoptosis by increasing BCL-2 and decreasing BAX. All these results suggested that NTS played very important and complex functions in EEC apoptosis. Notably, NTS also increased Caspase-3, FAS, and PTN and decreased SP1 in EECs *in vitro*. This difference may have been because NTS prevented EEC apoptosis, which was contrary to normal processes. Thus, we hypothesized that miR-181a plays a role in the regulation of endometrium cell apoptosis by downregulating NTS in EECs of dairy goats. Furthermore, NTS resulted in an increase in some biochemical markers of the RE, including LIF,

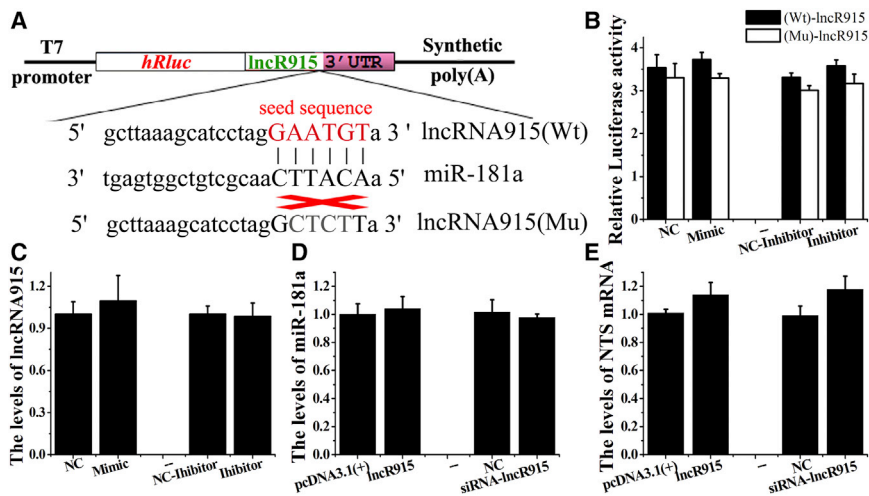


**Figure 6. IncR915 Was Not a Target of miR-181a in EECs**

(A) Schematic diagram illustrating the design of luciferase reporters with the Wt-IncR915 or the site-directed mutant (Mu-IncR915). The nucleotides in red represent the "seed sequence" of miR-181a, and the mutation nucleotides are in gray. (B) The IncR915 luciferase reporter vectors were co-transfected with miR-181a mimic (or negative control) into 293T cells; luciferase assay was performed 24 h after transfection. (C) miR-181a did not regulate the IncR915 levels in EECs; IncR915 levels were measured by qRT-PCR and normalized to GAPDH. (D) IncR915 did not regulate the miR-181a levels in EECs. (E) IncR915 did not regulate the NTS mRNA levels in EECs. Each experiment was repeated three times in triplicate, and the results are represented as mean  $\pm$  SD ( $n = 3$ ).

COX2, and HOXA10 in EECs *in vitro*, suggesting that NTS contributed to the formation of endometrial receptivity.

In conclusion, this study provides direct evidence demonstrating that ciR8073 could function as a ceRNA, which sequestered miR-181a, thereby protecting NTS transcripts from miR-181a-mediated suppression (Figure 11). As it was well established that NTS could promote EEC proliferation and increase the protein levels of some biochemical markers of RE, these data suggested that ceRNA regulation was of crucial importance in the formation of endometrial receptivity in dairy goats. This study facilitates the understanding of the role of ceRNAs in the regulatory mechanism of the RE and helps improve the understanding of the molecular regulation of endometrial receptivity.

## MATERIALS AND METHODS

### Ethics Statement

All animals in this study were maintained according to the No. 5 proclamation of the Ministry of Agriculture, P.R. China. And animal protocols were approved by the Review Committee for the Use of Animal Subjects of Northwest A&F University.

### Study Design and Tissue Collection

A total of 20 healthy 24-month-old multiparous dairy goats (Xinong Saanen) were induced to estrous synchronization for this study. The first day of mating was considered to be day 0 of pregnancy; D5 (PE) and D15 (RE) were important time points for the embryo implantation in goats.<sup>42</sup> The goats were euthanized when the goats lost consciousness caused by intravenous injection of barbiturate (30 mg/kg) in the PE and RE. Endometrium samples were obtained from the anterior wall of the uterine cavity. All tissue samples were washed briefly with PBS and then immediately frozen in liquid nitrogen.

### miRNA and Transcript Differential Expression Analysis

miRNA library construction, sequencing, and identification of potential novel miRNAs were shown as before.<sup>8</sup> Expression levels of all of

the transcripts, including putative mRNAs, lncRNAs, and circRNAs, were quantified as fragments per kilobase of exon per million fragments mapped (FPKM) using the Cuffdiff program from the Cufflinks package.<sup>7</sup> Differential gene expression was determined using Cuffdiff with a  $p$  value of  $< 0.05$ .

### Construction of ceRNA Network

The putative miRNA-mRNA, miRNA-lncRNA, and miRNA-circRNA interactions were evaluated using the algorithms of Targetscan version 6.2 (<http://www.targetscan.org/>) and miRanda version 3.3a (<http://www.microrna.org/microrna/home.do>). The miRNA binding-site prediction in lncRNAs was based on their full-length sequence in consideration of their non-coding properties. High-confidence miRNA-mRNA/-lncRNA/-circRNA pairs had a Targetscan context + score percentile  $> 50$  and miRanda max energy  $< -20$ . The ceRNA relationships were integrated using an in-house Perl script. The information including all of the above interactions was imported into Cytoscape software version 2.8.0 (<https://cytoscape.org/>) to construct a regulatory network.

### Vector Construction

Bioinformatic analysis of miRNA binding sequences in NTS, ciR8073, and ncR915 were performed to identify the target genes of miR-181a using miRanda and Targetscan. To construct reporters for luciferase assays, 3' UTR of NTS, ciR8073, and IncR915, respectively, containing the miR-181a target site were cloned and inserted downstream of the Renilla luciferase gene in the psiCHECK-2 vector (Promega, Madison, USA), and the mutated plasmids were constructed.

To construct reporters for overexpression assays, the coding domain sequence (CDS) of NTS, full length of ciR8073 and IncR915 were cloned and inserted in the psiDNA3.1(+) vector (Promega, Madison, USA), and the target site of miR-181a were mutated and constructed mutant psiDNA3.1(+)-ciR8073(Mu) and psiDNA3.1(+)-IncR915(Mu).

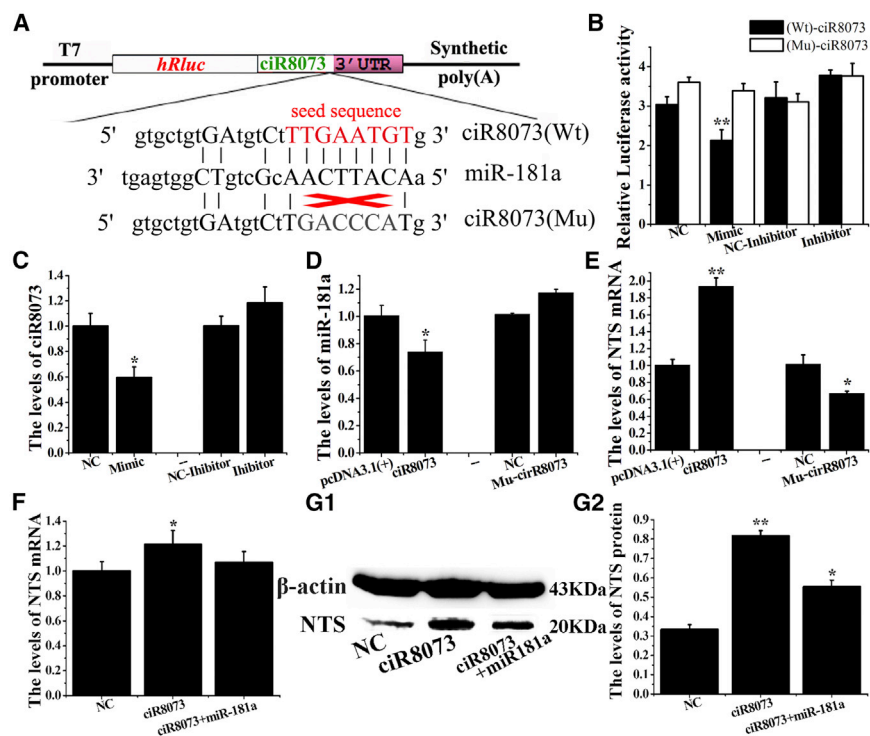


**Figure 7. Decreased Levels of miR-181a Served as a miRNA Sponge in EECs**

(A) Schematic diagram illustrating the design of luciferase reporters with the Wt-ciR8073 or the site-directed mutant (Mu-ciR8073). The nucleotides in red represent the "seed sequence" of miR-181a, and the mutation nucleotides are in gray. (B) The ciR8073 or its mutation luciferase reporter vectors were co-transfected with miR-181a mimic (or negative control) into 293T cells; luciferase assay was performed 24 h after transfection. (C) miR-181a decreased the ciR8073 levels in EECs; the levels were measured by qRT-PCR and normalized to GAPDH. (D) The miR-181a levels in EECs were overexpressed or mutational ciR8073 (Mu-ciR8073). (E) The NTS mRNA levels in EECs were overexpressed or mutational ciR8073 (Mu-ciR8073). (F) The NTS mRNA levels in EECs were overexpressed ciR8073 and miR-181a. (G) NTS protein levels in EECs were overexpressed ciR8073 and miR-181a; the densitometry was normalized to the  $\beta$ -actin density from the same lane. Each experiment was repeated three times in triplicate. \* $p < 0.05$ , \*\* $p < 0.01$ .

#### Luciferase Assay

The wild-type (psiCHECK-2-Wt) or mutated (psiCHECK-2-Mu) plasmids were co-transfected with the miR-181a mimic into 293T cells, respectively. At 24 h post-transfection, firefly (hLuc+) and Renilla (hRluc) luciferase activities were measured with the Dual-Glo luciferase assay system (Promega, USA). Experiments were performed three times.

#### RNA Extraction and qRT-PCR

Total RNA was extracted using Trizol reagent (TaKaRa, Dalian, China), and qRT-PCR was performed using SYBR Green PCR Master Mix (TaKaRa, Dalian, China) in a 20  $\mu$ L reaction. Glyceraldehyde-3-phosphate dehydrogenase (GAPDH) was used as the reference for mRNA and U6 for miR-181a, and all primers for qRT-PCR are shown in Table S1. The relative expression levels were calculated using the equation  $N = 2^{-\Delta\Delta Ct}$ .

Another total RNA was incubated for 15 min at 37°C with or without (mock) 3 U/ $\mu$ g of RNase R (Epicenter Biotechnologies, Chicago, USA). To quantify the amount of circRNA, cDNA was synthesized with the Prime Script RT reagent kit with genomic DNA (gDNA) Eraser (TaKaRa, Dalian, China) using random hexamers. In particular, the divergent primers annealing at the distal ends of circRNA were used to determine the abundance of circRNA, and the outward-facing primer sets are listed in Table S1.

#### Protein Extraction and WB Analysis

Protein extraction was performed as described previously.<sup>45</sup> Thirty micrograms of protein from each treatment was used for 12% SDS-PAGE and transferred onto nitrocellulose membranes (Millipore, Bedford, MA, USA) at 100 V for 1.5 h in an ice bath.

#### Primary Cell Culture and Purification

Primary EECs were isolated and purified by digestion of trypsin, centrifugation, and difference tempo adherence and observed by light microscope. Cell purity and identification was evaluated immunocytochemically as previously described.<sup>43</sup> The cells were cultured to the third generation with the same cell culture system to further purify the cells.

#### Cell Transfection

Mature miR-181a mimics, inhibitors, and siRNA-NTS were synthesized by GenePharma (Shanghai, China). Cells were plated at a density of  $7.5 \times 10^5$  in 6-well plates, then the cells were transfected at 50% confluency with miR-181a mimics, miR-181a inhibitors, NC, or NC inhibitors at final concentrations of 100 nM using the X-tremeGENE siRNA Transfection Reagent (Roche, Switzerland) according to the manufacturer's concentrations of 100 nM using the X-tremeGENE Lip2000 liposome (Invitrogen, USA).

#### Cell Proliferation and Apoptosis Assays

The MTT (Sigma, St. Louis, MO, USA) colorimetric assay was used to screen for cell proliferation as previously described.<sup>44</sup> To further investigate cell proliferation, a cell cycle staining kit was used (Liankebio, Hangzhou, China) according to the manufacturer's instructions. Cell apoptosis analysis was carried out using the Annexin-V-FITC and propidium iodide (PI) apoptosis kit, Annexin-V-positive and PI-negative cells were defined as early-apoptotic cells, and the late-apoptotic cells were Annexin-V- and PI-positive cells. Analyses were performed using a flow cytometer (BD Biosciences, San Diego, CA).



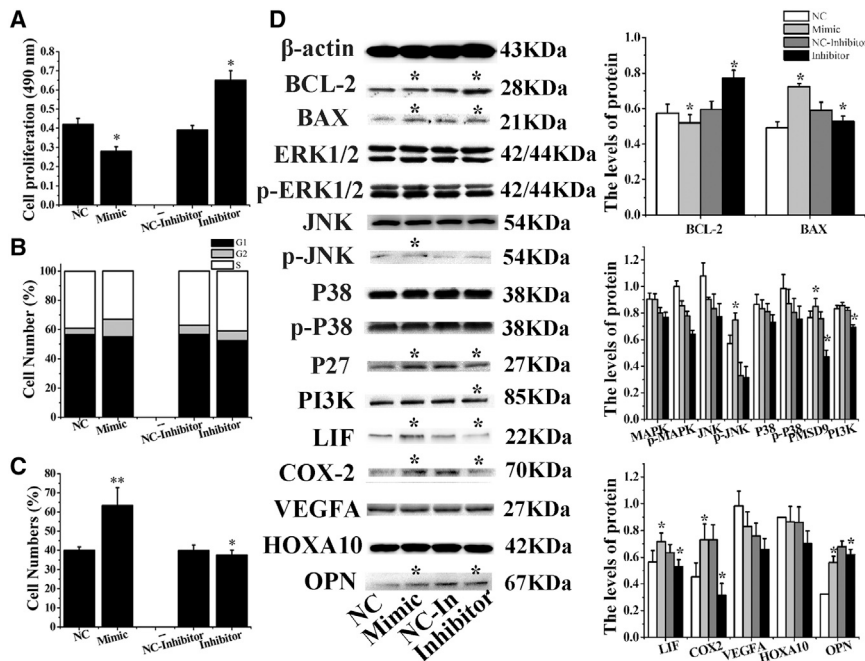


**Figure 8. miR-181a Promoted EECs Apoptosis In Vitro**

(A) The effect of miR-181a on the proliferation of EECs that were measured by MTT. Values were shown as means  $\pm$  SD (n = 7). The cell cycle (B) and apoptosis (C) analysis of EECs were detected with FCM. (D) The levels of BCL-2, BAX, MAPK pathway proteins, and endometrial receptivity markers (LIF, COX2, VEGFA, HOXA10, and OPN) were measured by WB after the EECs were treated with miR-181a. Densitometry was normalized to the  $\beta$ -actin density from the same lane; \*\*p < 0.01, \*p < 0.05.

was performed using the Quantity One program (Bio-Rad, California, USA). The experiments were performed three times.

#### IHC

For IHC, the paraffin-embedded tissue sections were de-paraffinized in xylene for 15 min and rehydrated in descending concentrations of ethanol (anhydrous ethanol for 5 min, 85% for 5 min, 75% for 5 min, and then rinsed with distilled water). Antigen retrieval in sodium citrate

buffer (pH = 9.0) was performed for 10 min in a microwave oven, then the tissue sections were placed in PBS (pH = 7.4) and washed three times (each time 5 min) on a decoloring shaking bed. Endogenous peroxidases of IHC were inhibited by incubation with 3% hydrogen peroxide for 25 min at RT. The samples were blocked in 5% BSA for 30 min, incubated with a primary antibody (as be shown in Table S2) at 4°C overnight, and then washed three times (each time 5 min) on a decoloring shaking bed. Then, the samples were incubated with HRP-labeled secondary antibody for 30 min at 37°C. After washing the cells three times in PBS, the color reaction was developed

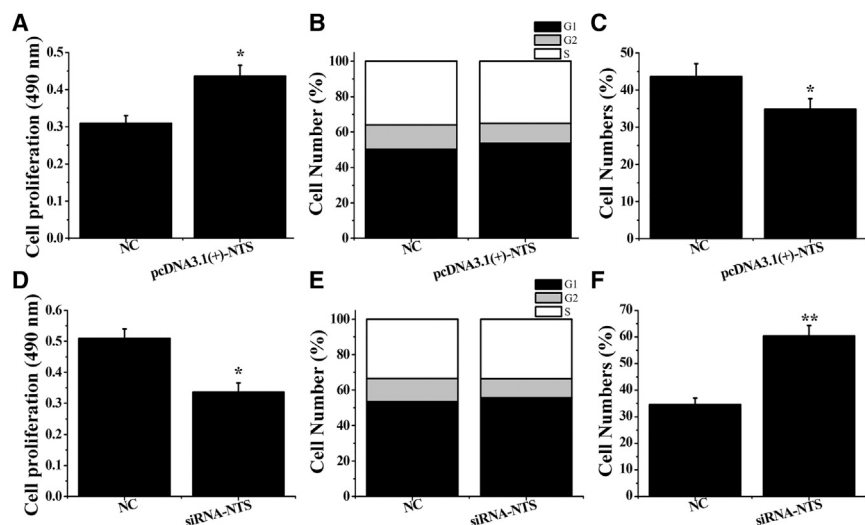


**Figure 9. NTS Inhibited EECs Apoptosis In Vitro**

Overexpressed NTS markedly promoted proliferation of EECs (A), did not change the cell cycle (B), and inhibited EEC apoptosis (C). siRNA-NTS significantly inhibited proliferation of EECs (D), did not change the cell cycle (E), and dramatically induced EEC apoptosis (F). Values were shown as means  $\pm$  SD (n = 7). The cell cycle (B and E) and apoptosis (C and F) analysis of EECs were detected with FCM. \*\*p < 0.01, \*p < 0.05.

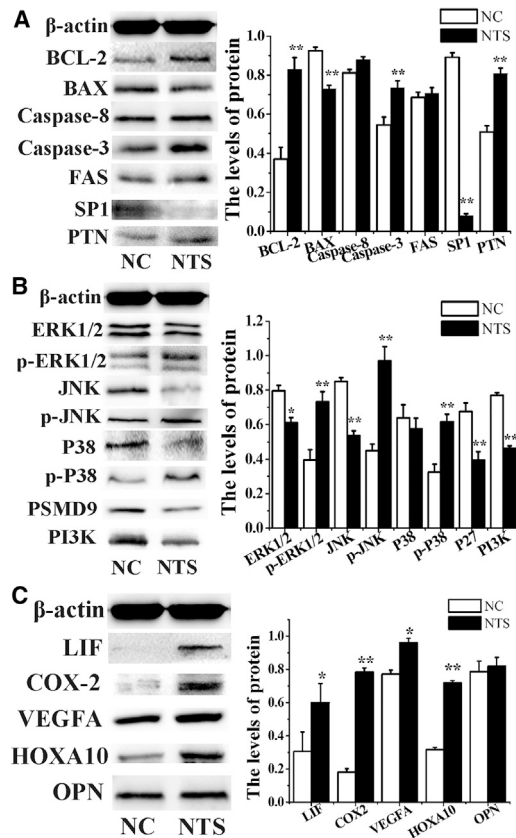


**Figure 10. NTS Increased the Expression Levels of BCL-2/BAX and Increased LIF, COX2, VEGFA, and HOXA10 in EECs *In Vitro***  
 The levels of apoptosis-related proteins (A) (BCL-2, BAX, Caspase-8, Caspase-3, FAS, SP1, and PTN), MAPK pathway proteins (B), and endometrial receptivity markers (C) (LIF, COX2, VEGFA, HOXA10, and OPN) were measured by WB when the NTS was overexpressed in EECs. Densitometry was normalized to the  $\beta$ -actin density from the same lane. \*\* $p < 0.01$ , \* $p < 0.05$ .

with the substrate diaminobenzidine according to the manufacturer's instructions, and the slides were washed under running water for 5 min before being counterstained with hematoxylin (Carnaxide, Oeiras, Portugal). After re-dyeing the nucleus with hematoxylin and ammonia, the slides were dehydrated with concentrations of ethanol and sealed with xylene for 5 min. The relative density of the positive cells (density/area) in each slide was analyzed using Image-Pro Plus 6.0 Software (Media Cybernetics, USA).

### MISH

An oligonucleotide probe complementary to the miR-181a sequence was purchased from RiboBio (Guangzhou, China). The sequence of the probe was 5e 5'-ACTCACCGACAGCGTTGAAGA-3TCACCGACAGCGTTGAAGA-3' (China). The sequence digoxigenin (DIG) and some of these bases were modified with a DIG-labeled LNA (locked nucleic acid). *In situ* hybridization for miR-181a (MISH) was performed on fixed paraffin-embedded sections as previously described.<sup>46</sup> The relative density of the positive cells (density/area)

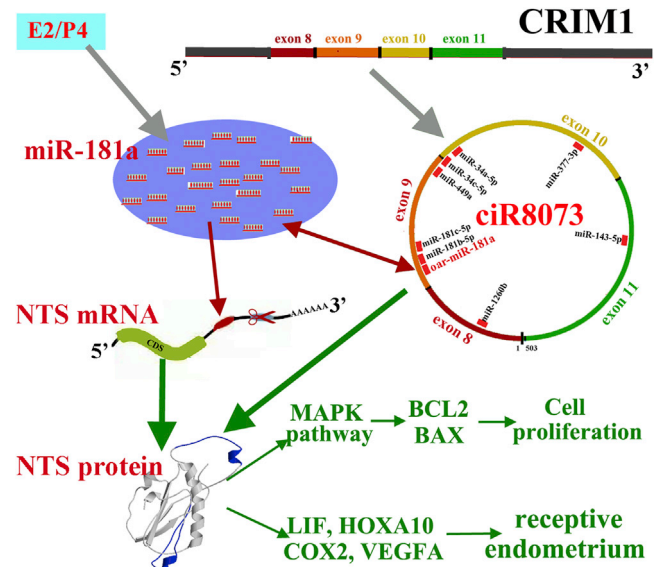


**Figure 11. Proposed Network of ciR8073-miR181a-NTS in the Endometrium of Dairy Goats**

ciR8073 regulates EECs by functioning as a ceRNA, which sequesters miR-181a, thereby relieving its repressive effect on NTS.

in each slide was analyzed using Image-Pro Plus 6.0 Software (Media Cybernetics, USA).

### Statistical Analysis

All the data were processed with SPSS 17.0 (SPSS, Chicago, IL, USA). One-way ANOVA was used to compare the differences, and the method of the least significant difference (LSD) was used for further analysis. Differences were considered significant when the p value was  $< 0.05$  (\*) and very significant when the p value was  $< 0.01$  (\*\*).

### SUPPLEMENTAL INFORMATION

Supplemental Information includes two tables, ten figures, and twelve data files can be found with this article online at <https://doi.org/10.1016/j.omtn.2018.12.005>.

### AUTHOR CONTRIBUTIONS

L.Z., X.L., S.C., and J.C. gathered samples, conceived the report, participated in its design, performed data analysis, interpreted results, and wrote the manuscript. L.Z., X.L., S.C., J.C., and X.M. participated in intellectual discussion. L.Z., X.L., and X.A. contributed to gathering samples. L.Z., Y.S., and B.C. designed experiments, analyzed data. All authors read and approved the final manuscript and declare no competing interests.

### CONFLICTS OF INTEREST

The authors declare no competing interests.

### ACKNOWLEDGMENTS

This study was supported by the PhD research startup foundation of Northwest A&F University (00400/Z109021811), the National Key

R&D Program of China (2016YFD0500508), Nature Science Foundation of Shaanxi Provincial (2015JM3087), and the Shaanxi Science and Technology Innovation Project Plan (2015KTCQ03-08 and 2016KTZDNY02-04). The funders had no role in study design, data collection and analysis, decision to publish, or preparation of the manuscript.

## REFERENCES

- Revel, A., Achache, H., Stevens, J., Smith, Y., and Reich, R. (2011). MicroRNAs are associated with human embryo implantation defects. *Hum. Reprod.* 26, 2830–2840.
- Altmäe, S., Martínez-Conejero, J.A., Esteban, F.J., Ruiz-Alonso, M., Stavreus-Evers, A., Horcajadas, J.A., and Salumets, A. (2013). MicroRNAs miR-30b, miR-30d, and miR-494 regulate human endometrial receptivity. *Reprod. Sci.* 20, 308–317.
- Macklon, N.S., Stouffer, R.L., Giudice, L.C., and Fauser, B.C. (2006). The science behind 25 years of ovarian stimulation for in vitro fertilization. *Endocr. Rev.* 27, 170–207.
- Shahandeh, A. (2013). Molecular mechanisms of oncogenic long non-coding RNAs. *Bioscience Research* 10, 38–54.
- Thum, T., and Condorelli, G. (2015). Long noncoding RNAs and microRNAs in cardiovascular pathophysiology. *Circ. Res.* 116, 751–762.
- Zhou, J., Xiong, Q., Chen, H., Yang, C., and Fan, Y. (2017). Identification of the Spinal Expression Profile of Non-coding RNAs Involved in Neuropathic Pain Following Spared Nerve Injury by Sequence Analysis. *Front. Mol. Neurosci.* 10, 91.
- Wang, Y., Xue, S., Liu, X., Liu, H., Hu, T., Qiu, X., Zhang, J., and Lei, M. (2016). Analyses of Long Non-Coding RNA and mRNA profiling using RNA sequencing during the pre-implantation phases in pig endometrium. *Sci. Rep.* 6, 20238.
- Song, Y., An, X., Zhang, L., Fu, M., Peng, J., Han, P., Hou, J., Zhou, Z., and Cao, B. (2015). Identification and profiling of microRNAs in goat endometrium during embryo implantation. *PLoS ONE* 10, e0122202.
- Wang, Y., Hu, T., Wu, L., Liu, X., Xue, S., and Lei, M. (2017). Identification of non-coding and coding RNAs in porcine endometrium. *Genomics* 109, 43–50.
- He, Q., Tian, L., Jiang, H., Zhang, J., Li, Q., Sun, Y., Zhao, J., Li, H., and Liu, M. (2017). Identification of laryngeal cancer prognostic biomarkers using an inflammatory gene-related, competitive endogenous RNA network. *Oncotarget* 8, 9525–9534.
- Yan, B., Yao, J., Liu, J.Y., Li, X.M., Wang, X.Q., Li, Y.J., Tao, Z.F., Song, Y.C., Chen, Q., and Jiang, Q. (2015). lncRNA-MIAT regulates microvascular dysfunction by functioning as a competing endogenous RNA. *Circ. Res.* 116, 1143–1156.
- Ma, M.Z., Chu, B.F., Zhang, Y., Weng, M.Z., Qin, Y.Y., Gong, W., and Quan, Z.W. (2015). Long non-coding RNA CCAT1 promotes gallbladder cancer development via negative modulation of miRNA-218-5p. *Cell Death Dis.* 6, e1583.
- Cesana, M., Cacchiarelli, D., Legnini, I., Santini, T., Sthandier, O., Chinappi, M., Tramontano, A., and Bozzoni, I. (2011). A long noncoding RNA controls muscle differentiation by functioning as a competing endogenous RNA. *Cell* 147, 358–369.
- Hansen, T.B., Jensen, T.I., Clausen, B.H., Bramsen, J.B., Finsen, B., Damgaard, C.K., and Kjems, J. (2013). Natural RNA circles function as efficient microRNA sponges. *Nature* 495, 384–388.
- Memczak, S., Jens, M., Elefsinioti, A., Torti, F., Krueger, J., Rybak, A., Maier, L., Mackowiak, S.D., Gregersen, L.H., Munschauer, M., et al. (2013). Circular RNAs are a large class of animal RNAs with regulatory potency. *Nature* 495, 333–338.
- Li, F., Zhang, L., Li, W., Deng, J., Zheng, J., An, M., Lu, J., and Zhou, Y. (2015). Circular RNA ITCH has inhibitory effect on ESCC by suppressing the Wnt/ $\beta$ -catenin pathway. *Oncotarget* 6, 6001–6013.
- Zhang, L., An, X.P., Liu, X.R., Fu, M.Z., Han, P., Peng, J.Y., Hou, J.X., Zhou, Z.Q., Cao, B.Y., and Song, Y.X. (2015). Characterization of the Transcriptional Complexity of the Receptive and Pre-receptive Endometria of Dairy Goats. *Sci. Rep.* 5, 14244.
- de Giorgio, A., Krell, J., Harding, V., Stebbing, J., and Castellano, L. (2013). Emerging roles of competing endogenous RNAs in cancer: insights from the regulation of PTEN. *Mol. Cell. Biol.* 33, 3976–3982.
- Karreth, F.A., and Pandolfi, P.P. (2013). ceRNA cross-talk in cancer: when ce-bling rivalries go awry. *Cancer Discov.* 3, 1113–1121.
- Su, L., Liu, R., Cheng, W., Zhu, M., Li, X., Zhao, S., and Yu, M. (2014). Expression patterns of microRNAs in porcine endometrium and their potential roles in embryo implantation and placentation. *PLoS ONE* 9, e87867.
- Zhang, Q., Zhang, H., Jiang, Y., Xue, B., Diao, Z., Ding, L., Zhen, X., Sun, H., Yan, G., and Hu, Y. (2015). MicroRNA-181a is involved in the regulation of human endometrial stromal cell decidualization by inhibiting Krüppel-like factor 12. *Reprod. Biol. Endocrinol.* 13, 23.
- Sakumoto, R., Hayashi, K.G., Saito, S., Kanahara, H., Kizaki, K., and Iga, K. (2015). Comparison of the global gene expression profiles in the bovine endometrium between summer and autumn. *J. Reprod. Dev.* 61, 297–303.
- Arai, M., Yoshioka, S., Nishimura, R., and Okuda, K. (2014). FAS/FASL-mediated cell death in the bovine endometrium. *Anim. Reprod. Sci.* 151, 97–104.
- Otsuki, Y. (2001). Apoptosis in human endometrium: apoptotic detection methods and signaling. *Med. Electron Microsc.* 34, 166–173.
- Heryanto, B., and Rogers, P.A. (2002). Regulation of endometrial endothelial cell proliferation by oestrogen and progesterone in the ovariectomized mouse. *Reproduction* 123, 107–113.
- Wasowska, B., Ludkiewicz, B., Stefańczyk-Krzybowska, S., Grzegorzewski, W., and Skipor, J. (2001). Apoptotic cell death in the porcine endometrium during the oestrous cycle. *Acta Vet. Hung.* 49, 71–79.
- Galán, A., O'Connor, J.E., Valbuena, D., Herrero, R., Remohí, J., Pampfer, S., Pellicer, A., and Simón, C. (2000). The human blastocyst regulates endometrial epithelial apoptosis in embryonic adhesion. *Biol. Reprod.* 63, 430–439.
- Liu, G., Li, Y., and Gao, X.G. (2016). microRNA-181a is upregulated in human atherosclerosis plaques and involves in the oxidative stress-induced endothelial cell dysfunction through direct targeting Bcl-2. *Eur. Rev. Med. Pharmacol. Sci.* 20, 3092–3100.
- Liu, C.Q., Yuan, Y., and Wang, Z.X. (2001). Effects of leukaemia inhibitory factor on endometrial receptivity and its hormonal regulation in rabbits. *Cell Biol. Int.* 25, 1029–1032.
- Miravet-Valenciano, J.A., Rincon-Bertolin, A., Vilella, F., and Simon, C. (2015). Understanding and improving endometrial receptivity. *Curr. Opin. Obstet. Gynecol.* 27, 187–192.
- Isayama, K., Zhao, L., Chen, H., Yamauchi, N., Shigeyoshi, Y., Hashimoto, S., and Hattori, M.A. (2015). Removal of Rev-erb $\beta$  inhibition contributes to the prostaglandin G/H synthase 2 expression in rat endometrial stromal cells. *Am. J. Physiol. Endocrinol. Metab.* 308, 2462–2467.
- Das, S.K., Chakraborty, I., Wang, J., Dey, S.K., and Hoffman, L.H. (1997). Expression of vascular endothelial growth factor (VEGF) and VEGF-receptor messenger ribonucleic acids in the peri-implantation rabbit uterus. *Biol. Reprod.* 56, 1390–1399.
- Chakraborty, I., Das, S.K., and Dey, S.K. (1995). Differential expression of vascular endothelial growth factor and its receptor mRNAs in the mouse uterus around the time of implantation. *J. Endocrinol.* 147, 339–352.
- Demir, R., Yaba, A., and Huppertz, B. (2010). Vasculogenesis and angiogenesis in the endometrium during menstrual cycle and implantation. *Acta Histochem.* 112, 203–214.
- Zanatta, A., Rocha, A.M., Carvalho, F.M., Pereira, R.M.A., Taylor, H.S., Motta, E.L.A., Baracat, E.C., and Serafini, P.C. (2010). The role of the Hoxa10/HOXA10 gene in the etiology of endometriosis and its related infertility: a review. *J. Assist. Reprod. Genet.* 27, 701–710.
- Petracco, R., Grechukhina, O., Popkhadze, S., Massasa, E., Zhou, Y., and Taylor, H.S. (2011). MicroRNA 135 regulates HOXA10 expression in endometriosis. *J. Clin. Endocrinol. Metab.* 96, E1925–E1933.
- Horcajadas, J.A., Riesewijk, A., Domínguez, F., Cervero, A., Pellicer, A., and Simón, C. (2004). Determinants of endometrial receptivity. *Ann. N Y Acad. Sci.* 1034, 166–175.
- Harada, T., Kaponis, A., Iwabe, T., Taniguchi, F., Makrydimas, G., Sofikitis, N., Paschopoulos, M., Paraskevaidis, E., and Terakawa, N. (2004). Apoptosis in human endometrium and endometriosis. *Hum. Reprod. Update* 10, 29–38.
- Iwahori, S., Yasui, Y., Kudoh, A., Sato, Y., Nakayama, S., Murata, T., Isomura, H., and Tsurumi, T. (2008). Identification of phosphorylation sites on transcription factor

- Sp1 in response to DNA damage and its accumulation at damaged sites. *Cell. Signal.* 20, 1795–1803.
40. Muramatsu, T. (2002). Midkine and pleiotrophin: two related proteins involved in development, survival, inflammation and tumorigenesis. *J. Biochem.* 132, 359–371.
41. Mansouri-Attia, N., Aubert, J., Reinaud, P., Giraud-Delville, C., Taghouti, G., Galio, L., Everts, R.E., Degrelle, S., Richard, C., Hue, I., et al. (2009). Gene expression profiles of bovine caruncular and intercaruncular endometrium at implantation. *Physiol. Genomics* 39, 14–27.
42. Igwebuike, U.M. (2009). A review of uterine structural modifications that influence conceptus implantation and development in sheep and goats. *Anim. Reprod. Sci.* 112, 1–7.
43. Pierro, E., Minici, F., Alesiani, O., Miceli, F., Proto, C., Screpanti, I., Mancuso, S., and Lanzone, A. (2001). Stromal-epithelial interactions modulate estrogen responsiveness in normal human endometrium. *Biol. Reprod.* 64, 831–838.
44. Sun, X., He, Y., Ma, T.-T., Huang, C., Zhang, L., and Li, J. (2014). Participation of miR-200a in TGF- $\beta$ 1-mediated hepatic stellate cell activation. *Mol. Cell. Biochem.* 388, 11–23.
45. Subramaniam, K.S., Omar, I.S., Kwong, S.C., Mohamed, Z., Woo, Y.L., Mat Adenan, N.A., and Chung, I. (2016). Cancer-associated fibroblasts promote endometrial cancer growth via activation of interleukin-6/STAT-3/c-Myc pathway. *Am. J. Cancer Res.* 6, 200–213.
46. Li, J., Yang, H., Li, Y., Liu, Y., Chen, S., Qi, C., Zhang, Q., Lan, T., He, X., Guan, X.Y., and Wang, L. (2014). microRNA-146 up-regulation predicts the prognosis of non-small cell lung cancer by miRNA in situ hybridization. *Exp. Mol. Pathol.* 96, 195–199.